Structure and Mass Analysis of 14S Dynein Obtained from *Tetrahymena* Cilia

Silvio P. Marchese-Ragona,* Joseph S. Wall,‡ and Kenneth A. Johnson

*Department of Molecular and Cell Biology, Pennsylvania State University, University Park, Pennsylvania 16802; and ‡Department of Biology, Brookhaven National Laboratory, Upton, New York 11973

Abstract. Scanning transmission electron microscopic analysis revealed that the 14S fraction of *Tetrahymena* dynein was of a mixture of two types of particles in approximately equal proportions. The 14S dynein molecules were roughly ellipsoid in shape with approximate axes of 9.5 and 14.5 nm. About half of the particles had tails 20–24-nm long. By the integration of electron scattering intensities, particles with tails had an average mass of 510 kD with a SD of 90 kD. The globular heads of both types of particles had an average mass of 330 kD with a SD of 60 kD. The mass of the tail structure was about 180 kD. By SDS-PAGE, the 14S dynein consisted of two high molecular mass polypeptides above 300 kD that could be distinguished by immunoblot analysis.

THE basis of ciliary and flagellar motility is the active sliding of the outer doublet microtubules. The sliding of the microtubules is mediated by the ATPase action of the dynein arms that decorate each doublet microtubule (Brokaw and Benedict, 1968; Gibbons and Gibbons, 1972; Gibbons, 1981). High salt extraction of *Tetrahymena* axonemes yields two ATPases which can be resolved by sucrose gradient sedimentation as 14S and 22S dyneins (Gibbons and Rowe, 1965). The 22S dynein is believed to originate solely from the outer dynein arm, although this has not been firmly established. The origin of the 14S dynein is even less certain, but may originate from the inner dynein arms, or from some other axonemal structure, such as the radial spokes (Nagano, 1965), or microtubule-membrane links (Dentler et al., 1980).

The structural and functional properties of 22S dynein have received considerable attention over the last few years; however, little is known about the 14S dynein. Previous analysis of *Tetrahymena* 22S dynein by scanning transmission electron microscopy (STEM)[1] provided the first evidence that dyneins consist of globular heads connected by flexible strands to a base (Johnson and Wall, 1983). Moreover, the STEM mass measurement, which identified the three-headed particle as single dynein molecules, suggested that the heads form the ATP-sensitive site of association with microtubules, and helped to relate the results on *Tetrahymena* with those obtained with *Chlamydomonas* dyneins (Witman et al., 1982). Therefore, it was hoped that STEM analysis of 14S dynein would be equally revealing. In this communication we report our findings of STEM analysis of *Tetrahymena* 14S dynein. We demonstrate for the first time that the 14S fraction of *Tetrahymena* dynein consists of two immunologically distinct polypeptides and two populations of particles that differ in their structures and masses.

1. *Abbreviation used in this paper*: STEM, scanning transmission electron microscopy.

Materials and Methods

Isolation of 14S Dynein

Dynein was obtained by high salt extraction of isolated demembranated axonemes from *Tetrahymena thermophila* (strain B-225, a mucus deficient mutant, was a gift from E. Orias, University of California at Santa Barbara, Santa Barbara, CA). The 14S dynein was purified by chromatography on DEAE-Sephacel and sucrose gradient fractionation as described previously (Porter and Johnson, 1983). Only the center of the 14S peak was taken from the sucrose gradient, although no significant differences in the polypeptide composition were observed in the leading or trailing edges when examined by SDS-PAGE. Sucrose gradient profiles were analyzed on a 5–15% acrylamide-gradient gel and visualized with Coomassie Brilliant Blue R-250. Rates of ATP hydrolysis for both 22S and 14S dynein were measured as the linear production of free P_i over the course of 30 min. Dynein (25 μg/ml) was incubated at 28°C with 1 mm ATP. 25 μl aliquots were removed at 10-min intervals and the reaction quenched with 2 N perchloric acid and stored on ice to reduce the rate on non-enzymatic hydrolysis of ATP. When all samples had been collected, they were assayed for P_i by the method of Lanzetta, et al. (1979). The specific activity of the 14S dynein was 0.05 μmole/mg/min, compared to a value of 0.16 μmole/mg/min for 22S dynein.

Preparation of Antibody

New Zealand white female rabbits were injected intracutaneously in several sites along their backs with 50–100 μg of 14S dynein in complete Freund's adjuvant (1:1, vol/vol). Two boosts with 50–100 μg of 14S dynein in incomplete Freund's adjuvant were given every 2 wk. Blood was taken 2 wk after the final injection.

Protein Blotting

For protein blotting of the heavy chains of 14S dynein, SDS-PAGE was performed according to the method of Laemmli (1970) using 3.0% acrylamide with a 0–8 M urea gradient. The conditions for the transfer of protein to nitrocellulose were similar to those described by King et al. (1985). Trans-

fers were performed on a TE 42 Transphor unit (Hoefer Scientific Instruments, San Francisco, CA) at 0.4 A for 30 min and then 1.5 A for three h. The nitrocellulose used had a pore size of 0.2 μm (BA-83; Shleicher and Schuell). After completion of the transfer procedure, the nitrocellulose blots were washed in distilled water, air dried, and stored at room temperature until use.

Affinity Purification

Nitrocellulose blots were stained with Amido Black (Talian et al., 1983) and strips containing the upper and lower high molecular mass polypeptides, termed HC1 and HC2, and a control blank strip were cut from the sheets. The Amido Black stain-destain procedure did not alter the antigenicity of the protein adsorbed to nitrocellulose. The strips of nitrocellulose were washed four times for 10 min in PBS containing 0.5% Tween 20 as the blocking agent, after which they were incubated overnight at 25°C with 14S dynein antisera diluted 1:500. Unbound antibody was removed by four 10-min washes in PBS plus 0.5% Tween 20.

The antibodies were eluted from the nitrocellulose strips by a 2-min incubation with 10 ml of 0.2 M glycine-HCl, pH 2.8. The eluted material was removed and immediately adjusted to pH 7.5 by the addition of 240 μl of 3 M Tris base.

Detection of Antigens Bound to Nitrocellulose Blots

Nitrocellulose blots of the heavy chains of 14S dynein were washed three times for 10 min in PBS plus 0.5% Tween before being incubated for 2 h at room temperature with either the 14S antiserum diluted 1:500 or the undiluted affinity purified antibodies.

Unreacted antibody was removed with 3 × 10-min washes of PBS plus 0.5% Tween 20, and incubated for a further 2 h at room temperature with a 1:1,000 dilution of goat anti-rabbit antibody conjugated to alkaline phos-

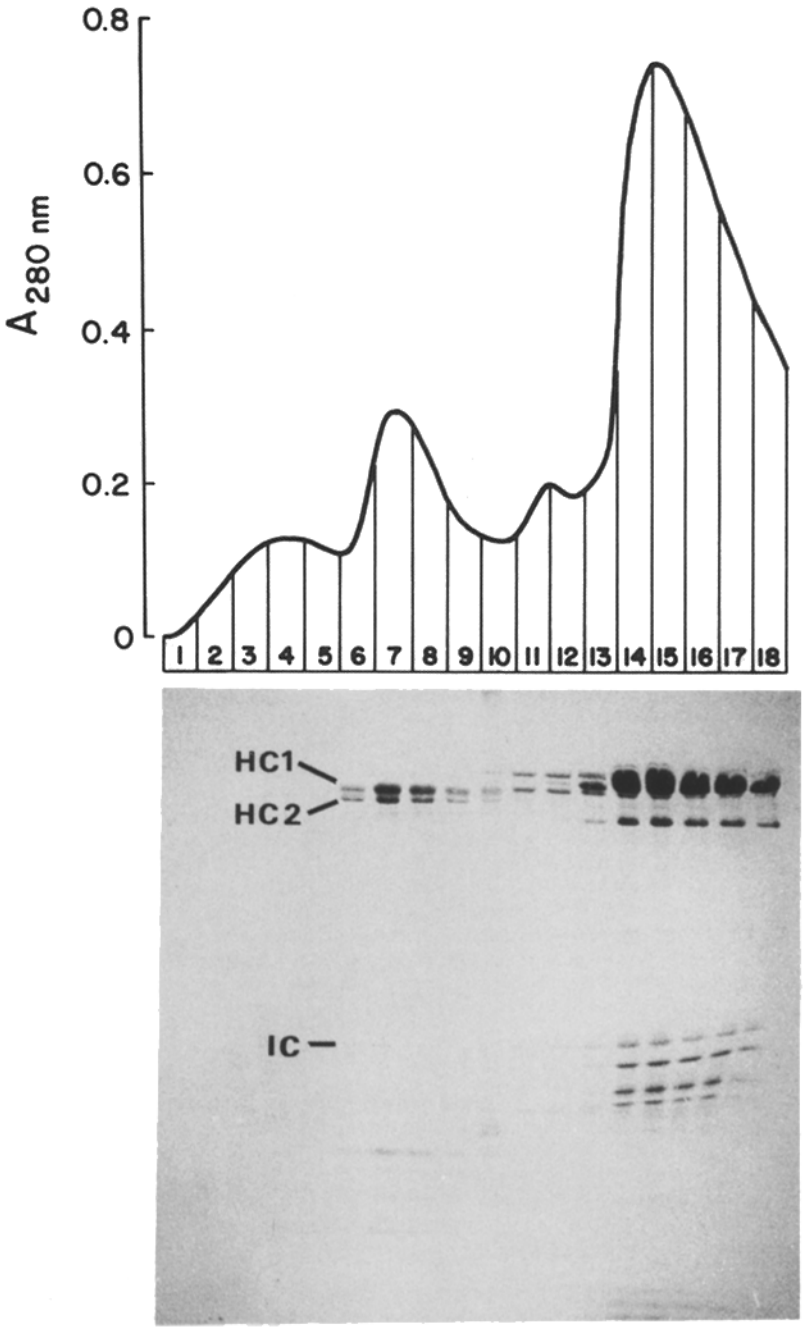

Figure 1. Sucrose gradient density profile of DEAE-Sephacel-column-purified dynein and corresponding SDS-PAGE analysis of each fraction. The 14S dynein (fractions 6–9) and 22S dynein (fractions 13–18) are well separated. No significant differences in the polypeptide compositions were seen in the leading and trailing edges of the 14S peak.

The 14S dynein consisted of two high molecular mass chains above 300 kD, designated HC1 and HC2, one intermediate chain, IC, with a molecular mass of 110 kD and three predominant light chains.

phatase. After an additional three 10-min washes in PBS plus 0.5% Tween 20, to remove unreacted goat anti-rabbit antibody, the nitrocellulose was washed once in 0.15 M Tris-acetate buffer (pH 9.5). The antibodies were detected on the nitrocellulose using 5-bromo-4-chloro-3-indolyl phosphate as the substrate and nitro blue tetrazolium, as the color reagent.

STEM Analysis

Specimens were prepared and imaged at the Brookhaven STEM Biotechnology Resource (Upton, NY). Samples of 14S dynein were diluted to a concentration of 30 μg/ml in 10 mM PIPES, 0.8 mM $MgCl_2$, pH 7.0, and applied to an electron microscope grid by injection into a droplet of buffer on a thin carbon foil supported by a holey carbon film. After 30 s, the grid was washed four times with buffer. Tobacco mosaic virus was added as a standard with a final wash step in water. The grids were then quickly frozen by plunging into nitrogen slush (−210°C), freeze-dried at −95°C and transferred under vacuum to the microscope stage.

The dose of electrons required for a single scan to be recorded was less than 2 electrons/A^2 and was sufficiently low to reduce mass loss to less than 1.0% (Mosesson et al., 1981). The use of tobacco mosaic virus particles as an internal standard largely compensated for this small loss.

The mass analysis was accomplished by integration of electron-scattering intensities of an area containing specimen, then subtracting the background. Only isolated particles were used for the mass analysis, and particles that appeared to be aggregated or juxtaposed to either another particle or a Tobacco mosaic virus were not used. For more specific information concerning the mass analysis, see Mosesson et al. (1981).

STEM

Thin carbon films that had been deposited on freshly cleaved mica were floated onto the surface of a solution containing 14S dynein at a concentration of 30 μg/ml in 10 mM PIPES, 0.8 mM $MgCl_2$. After several seconds, the carbon film was removed and floated onto the surface of 2% uranyl acetate.

The carbon films were picked up on uncoated 400 mesh copper grids, either by bringing the grid up from underneath the carbon film or by placing the grid on top of the carbon film.

The negatively stained preparations were viewed in a Philips 300 at 80 kv with a 30-μm objective aperture.

Results

SDS-PAGE analysis of the sucrose gradient profile of a typical dynein preparation is presented in Fig. 1. Fractions 6–9 contain 14S dynein, while fractions 12–18 contain 22S dynein. The 14S dynein fractions contain 2 heavy chains of greater than 300 kD (HC1 and HC2), one intermediate chain (IC), with a molecular mass of 110 kD, and approximately three light chains between 55 and 30 kD. By densitometry, HC1 was always in excess of HC2 accounting for 60–70% of the stain in the heavy chain region.

Immunoblot analysis showed that the two heavy chains of 14S dynein are immunologically distinct (Fig. 2). Affinity purified antibodies to HC1 did not cross react with HC2 (lane *2*), however a small amount of cross-reactivity was observed with antibodies affinity purified to HC2 (lane *3*).

By STEM, the 14S fraction of *Tetrahymena* dynein was a mixture of two types of globular particles in approximately equal proportions (Figs. 3 and 4). All of the particles had a globular region roughly ellipsoidal in shape with approximate axes of 9.5, and 14.5 nm. Slightly more than half the particles, 50–70% depending on the preparation had tails. The tail was 20–24-nm long also with the distal 5–10 nm more massive than the proximal part.

Negatively stained preparations of 14S dynein (Fig. 5), showed individual globular particles some with tails. The majority of the molecules had a stain accumulated in and around the center of the particle suggesting the presence of a pit or cleft in the molecule.

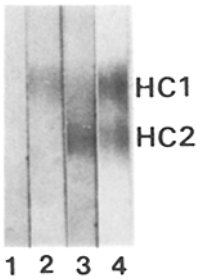

Figure 2. Immunoblot of the 14S heavy chains HC1 and HC2 separated on a 3% acrylamide, 0–8 M urea gradient gel. The control, lane *1*, was reacted with material eluted from a blank strip of nitrocellulose that had been incubated with a 1:500 dilution of 14S antiserum. Lane *2* was reacted with HC1 affinity purified antibodies. Lane *3* was reacted with HC2 affinity purified antibodies. Lane *4* was reacted with 1:500 dilution of antiserum.

Mass analysis of individual particles by the integration of electron scattering intensities gave partially overlapping distributions (Fig. 6). The average mass of particles with tails was 510 kD. The globular heads of both types of particles had an average mass of 330 kD. The mass of the tail structure was ~180 kD.

Discussion

The 14S fraction of *Tetrahymena* dynein consists of two distinctive heavy chains and two classes of particles, distinguishable by their morphologies and masses. The particles without the tails were lower in mass than those with tails. The mass showed that the tail was indeed missing and not just obscured or wrapped around the particle.

The simplest interpretation of the SDS–PAGE analysis and the STEM analysis is that the tail-less particle (mass = 330 kD) contains one copy of either HC1 or HC2, and probably very little of anything else. Whereas the tailed particle (mass = 510 kD) contains one copy of the remaining high molecular mass chain, one copy of the intermediate chain (mass = 110 kD) and one copy of each of the three light chains between 30–55 kD.

The results obtained here represent a refinement of a previous attempt to characterize the structure and mass of *Tetrahymena* 14S dynein by Gibbons and Rowe (1965) who used negative staining and unidirectional shadowing techniques to establish that 14S dynein was a globular particle roughly ellipsoid in shape, with approximate dimensions of 8.5, 9.0, and 14.0 nm. However, Gibbons and Rowe did not report any tail-like structures associated with the particles. This may have been due, in part, to the relatively low resolution of the shadowed preparations. Assuming an anhydrous protein density of 1.35 g/cm^3, Gibbons and Rowe estimated the molecular mass of 14S dynein to be 540 kD with a probable error of 20%. Using the short column sedimentation equilibrium method for determining molecular mass they obtained a value of 600 ± 100 kD for 14S dynein. Considering the potential for systematic errors in their estimates of molecular mass, the values reported by Gibbons and Rowe were quite close to the values reported here.

STEM mass analysis is ideally suited for the mass measurement of individual molecules and the domains of molecules. For example, STEM mass analysis (Johnson and Wall, 1983) gave an average mass measurement of 1.95 mD for the 22S dynein which has recently been confirmed by hydrody-

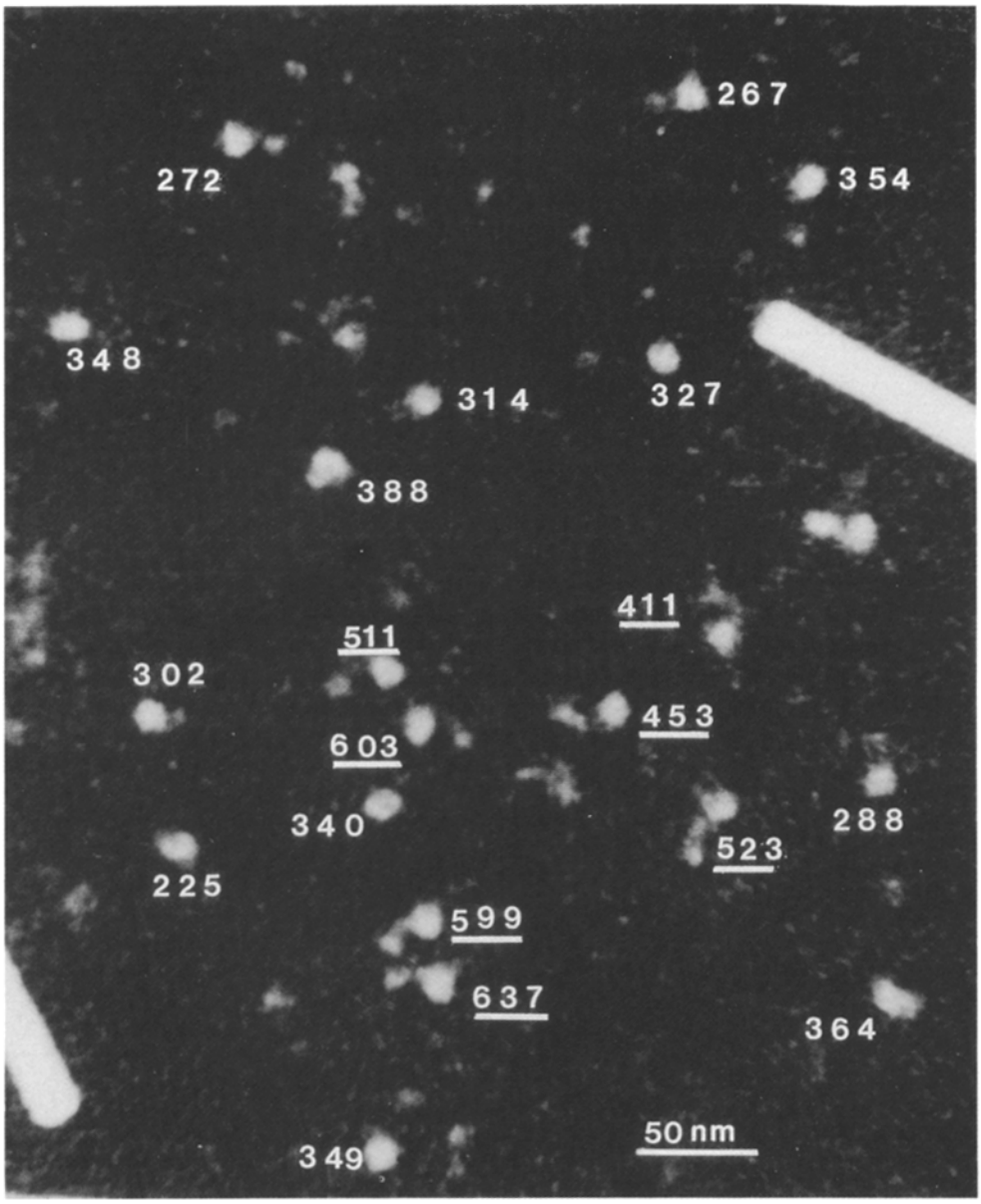

Figure 3. STEM of 14S dynein particles. Samples of unfixed, unstained 14S dynein were applied to a carbon film and freeze-dried and then examined in the Brookhaven STEM as described by Mosesson et al. (1981). The rod at the right of the micrograph is a tobacco mosaic virus particle used for internal mass calibration. The number next to each particle is its mass in kD. The underlined values are for particles which exhibited a tail that was included in the mass measurement.

namic and light scattering studies (Clutter et al., 1983, and manuscript in preparation).

The possibility that 14S dynein is a proteolytic product of 22S dynein has been ruled out on two accounts. Firstly, polyclonal antibodies against 22S dynein do not react with 14S dynein when assayed on immunoblots, or by solid phase ELISA's (data not shown). Secondly, proteolysis of 22S dynein does not yield any fragments that resemble 14S dynein when characterized by electron microscopy or SDS-PAGE (Clutter, D. B., and K. A. Johnson, unpublished results). Since HC1 and HC2 are immunologically distinguishable, the possibility that the tail-less particles are the proteolytic products of the larger tailed particles appears to be unlikely.

The possibility that all of the anti-HC1 antibodies are against a particular region of HC1 that is cleaved off to produce HC2 seems very remote, especially because the antiserum used for the affinity purification reacted strongly with every component of the 14S dynein fraction. Therefore, one would not expect that in such an antiserum, antibodies would be raised exclusively against a small 10–30-kD polypeptide and not against any of the remaining 300 kD polypeptide.

We have been unable to separate the two species of particles in the 14S fraction, using gel-filtration, HPLC, gradient centrifugation, and selective binding to microtubules, with and without maps, or in the presence and absence of ATP. Therefore, we are unable to say whether one or both particles possess ATPase activity.

Currently we do not know the origins of the two species of particles within the 14S dynein fraction. One possibility is that the two species of particles may have originated from a common larger dynein molecule, and may have broken down during the extraction procedure into smaller fragments; as is the case for *Chlamydomonas* outer and inner dynein arms (Piperno and Luck, 1979; 1981). Piperno and Luck (1981) obtained evidence suggesting that the inner arm of *Chlamydomonas* contained two separate ATPases that had

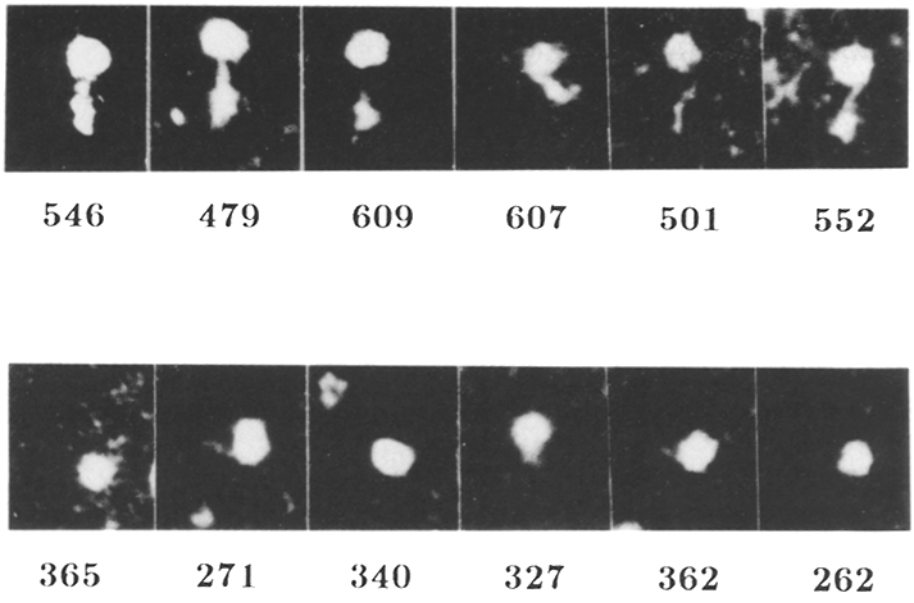

Figure 4. STEM Mass analysis of individual 14S particles. The mass, as measured by integration of electron scattering intensities, is given in kD beneath each particle. The top row shows particles that were selected as having a tail, whereas, the bottom row shows particles lacking the tail.

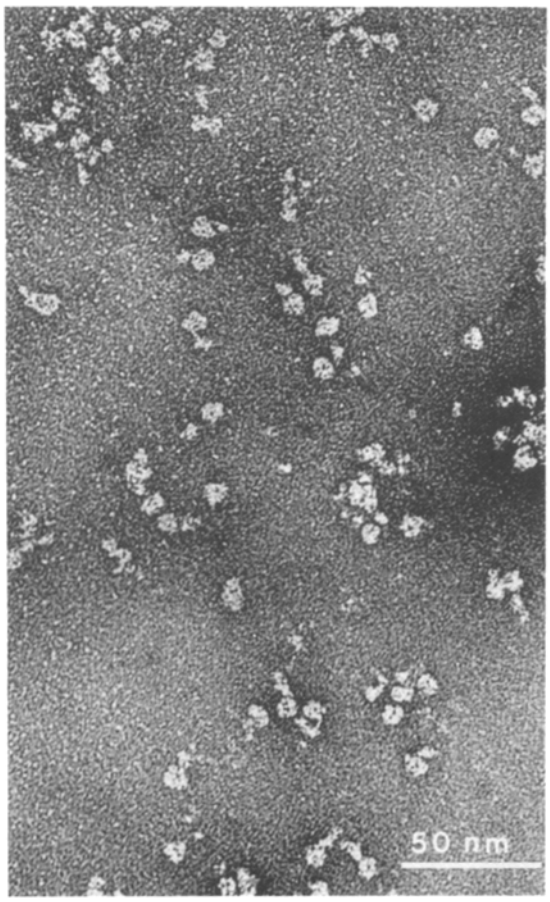

Figure 5. Negatively stained preparation of 14S dynein depicting globular particles with and without tail-like structures attached. A stain accumulation in the center of the globular particles suggests the presence of a pit or cleft in the molecule.

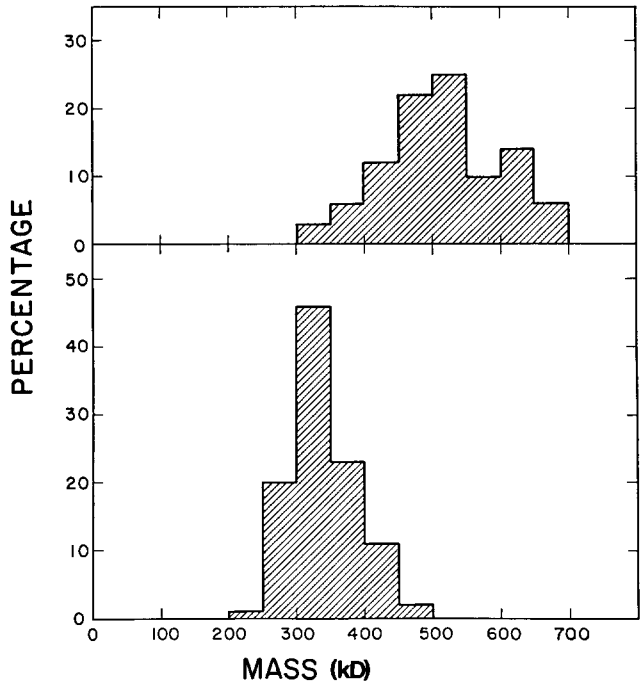

Figure 6. Distribution of particle masses. The histogram depicts the distribution of masses for particles with tails (*upper*) and without tails (*lower*). The average mass of particles with tails is 510 ± SD 90 kD and the average mass of particles without tails is 330 ± SD 60 kD.

sedimentation coefficients of 12.5 S and 10–11 S; and so, this result may be compatible with our current findings that *Tetrahymena* 14S dynein consists of two types of particles.

An alternative possibility is that the two types of particles do not originate from a common origin and are indeed two distinct species. In addition to the dynein arms, ATPase activity has been reported to be located within the region of the radial spoke head (Nagano, 1965), and the outer doublet membrane link (Dentler et al., 1980; Baccetti et al., 1979). Dentler et al. (1980) showed that the link between the outer doublet microtubule and the membrane in *Tetrahymena* was a dynein-like molecule with a sedimentation coefficient of 14S, and had a similar polypeptide composition to that of axonemal 14S dynein. In addition, the enzyme activity of microtubule-membrane link had nucleotide and divalent cation requirements similar to those of 14S dynein, as well as being inhibited by vanadate ions. Further work is underway to establish the origin of the two 14S particles by immunoelectron microscopy.

The authors wish to thank James Hainfeld, Kristen Chung, and Frank Kito for help in performing the STEM measurements and Kevin Facemyer for his outstanding technical assistance.

The work presented here was performed, in part, at the Brookhaven STEM, a National Institutes of Health Biotechnology Resource (Upton, NY) (RR00715).

This work was supported by National Institutes of Health grant GM32023. K. A. Johnson was supported by an Established Investigatorship of the American Heart Association and with funds contributed in part by the Pennsylvania Affiliate.

Received for publication 9 December 1986, and in revised form 21 September 1987.

References

Baccetti, B., A. G. Burrini, R. Dallai, and V. Pallini. 1979. The dynein electrophoretic bands in axonemes naturally lacking the inner or the outer arm. *J. Cell Biol.* 80:334–340.

Brokaw, C. J., and B. Benedict. 1968. Mechanochemical coupling in flagella. I. Movement dependent dephosphorylation of ATP by glycerinated spermatozoa. *Arch. Biochem. Biophys.* 125:770–778.

Clutter, D. B., D. Stimpson, V. A. Bloomfield, and K. A. Johnson. 1983. The structure of dynein in solution. *J. Cell Biol.* 97:197*a* (Abstr.)

Dentler, W. L., M. M. Pratt, and R. E. Stephens. 1980. Microtubule-membrane interactions in cilia: photochemical cross-linking of bridge structures and the identification of a membrane-associated dynein-like ATPase. *J. Cell Biol.* 84:381–403.

Gibbons, I. R. 1981. Cilia and flagella of eukaryotes. *J. Cell Biol.* 91:107*s*–124*s*.

Gibbons, B. H., and I. R. Gibbons. 1972. Flagellar movement and adenosine triphosphatase activity in sea urchin sperm extracted with Triton X-100. *J. Cell Biol.* 54:75–97.

Gibbons, I. R., and A. J. Rowe. 1965. Dynein: A protein with adenosine triphosphatase from cilia. *Science (Wash, DC).* 149:424–425.

Johnson, K. A., and J. S. Wall. 1983. Structure and molecular weight of the dynein ATPase. *J. Cell Biol.* 96:669–678.

King, S. M., T. Otter, and G. B. Witman. 1985. Characterization of monoclonal antibodies against *Chlamydomonas* flagellar dyneins by high resolution protein blotting. *Proc. Natl. Acad. Sci. USA.* 82:4717–4721.

Laemmli, V. K. 1970. Cleavage of structural proteins during assembly of the head of bacteriophage T4. *Nature (Lond.).* 227:680–685.

Lanzetta, P. A., L. J. Alvarez, P. S. Reinach, and O. A. Candia. 1979. Improved assay for nanomole amounts of inorganic phosphate. *Analyt. Biochem.* 100:95–97.

Mosesson, M. W., J. Hainfeld, J. Wall, and R. H. Haschemeyer. 1981. Identification and mass analysis of human fibrinogen molecules and their domains by scanning transmission electron microscopy. *J. Mol. Biol.* 153:695–718.

Nagano, T. 1965. Localization of adenosine triphosphatase activity in the rat sperm tail as revealed by electron microscopy. *J. Cell Biol.* 25:101–112.

Porter, M. E., and K. A. Johnson. 1983. Characterization of ATP-sensitive binding of *Tetrahymena* 30S dynein to bovine brain microtubules. *J. Biol. Chem.* 258:6575–6581.

Piperno, G., and D. J. L. Luck. 1979. Axonemal ATPases from flagella of *Chlamydomonas reinhardtii*: Purification of two dyneins. *J. Biol. Chem.* 254:3084–3090.

Piperno, G., and D. J. L. Luck. 1981. Inner arm dyneins from flagella of *Chlamydomonas reinhardtii*. *Cell.* 27:331–340.

Talian, J. C., J. B. Olmsted, and R. D. Goldman. 1983. A rapid procedure for preparing fluorescein-labeled specific antibodies from whole antiserum: Its use in analyzing cytoskeletal architecture. *J. Cell Biol.* 97:1277–1282.

Witman, G. B., K. A. Johnson, K. K. Pfister, and J. S. Wall. 1982. Fine structure and molecular weight of the outer arm dyneins of *Chlamydomonas*. *J. Submicros. Cytol.* 15:193–197.